ANNUAL REVIEWS

Annual Review of Microbiology

Structural Basis of Hydrogenotrophic Methanogenesis

Seigo Shima,[1] Gangfeng Huang,[1] Tristan Wagner,[2] and Ulrich Ermler[3]

[1]Max Planck Institute for Terrestrial Microbiology, 35043 Marburg, Germany; email: shima@mpi-marburg.mpg.de

[2]Max Planck Institute for Marine Microbiology, 28359 Bremen, Germany

[3]Max Planck Institute of Biophysics, 60438 Frankfurt am Main, Germany

Annu. Rev. Microbiol. 2020. 74:713–33

First published as a Review in Advance on July 21, 2020

The *Annual Review of Microbiology* is online at micro.annualreviews.org

https://doi.org/10.1146/annurev-micro-011720-122807

Keywords

methanogenesis, X-ray crystal structure, enzymes, coenzymes, prosthetic groups, metabolisms

Abstract

Most methanogenic archaea use the rudimentary hydrogenotrophic pathway—from CO_2 and H_2 to methane—as the terminal step of microbial biomass degradation in anoxic habitats. The barely exergonic process that just conserves sufficient energy for a modest lifestyle involves chemically challenging reactions catalyzed by complex enzyme machineries with unique metal-containing cofactors. The basic strategy of the methanogenic energy metabolism is to covalently bind C_1 species to the C_1 carriers methanofuran, tetrahydromethanopterin, and coenzyme M at different oxidation states. The four reduction reactions from CO_2 to methane involve one molybdopterin-based two-electron reduction, two coenzyme F_{420}–based hydride transfers, and one coenzyme F_{430}–based radical process. For energy conservation, one ion-gradient-forming methyl transfer reaction is sufficient, albeit supported by a sophisticated energy-coupling process termed flavin-based electron bifurcation for driving the endergonic CO_2 reduction and fixation. Here, we review the knowledge about the structure-based catalytic mechanism of each enzyme of hydrogenotrophic methanogenesis.

Contents

INTRODUCTION

In the anaerobic zone of ecosystems, anaerobic bacteria, fungi, and protozoa decompose polymeric organic material (e.g., cellulose) to monomeric (e.g., glucose) organic material. Fermenting bacteria complete the degradation process by releasing organic acids, H_2, and CO_2. Many of these simple molecules serve as substrates for methanogenic archaea, which convert them to methane (CH_4), the smallest organic compound. On Earth, 1 Gt of biological CH_4 is annually produced in anaerobic habitats, including oceans, ponds, paddy fields, and intestinal tracts of animals (mainly ruminants and insects) (88, 114). Moreover, CH_4 can be industrially produced by digesting organic wastes in biogas generators and then applied as a biofuel.

The formed CH_4 is oxidized back to CO_2 mainly by aerobic methanotrophic bacteria using O_2 as the final electron acceptor and anaerobic methanotrophic archaea (ANME) (79). Most of the residual CH_4 diffuses as inert gas into the atmosphere and is slowly degraded to CO_2 by photochemical reactions. Although the atmospheric concentration of CH_4 is ca. 1.8 ppm and that of CO_2 is ca. 400 ppm (114), one CH_4 molecule is considered to have a much stronger effect (~30-fold) on global warming and climate change than one molecule of CO_2 (117). In the last 100 years, the atmospheric CH_4 concentration has constantly increased (89). A small amount of the produced CH_4 is stored in deep-sea sediments as methane hydrate that accumulated over millions of years (5).

In this review, we describe the recent progress of research on the catalytic mechanism of enzymes involved in hydrogenotrophic methanogenesis based on the crystal structure of the enzyme–substrate complexes, as well as on enzymological and biophysical analyses of the enzymes.

OVERVIEW OF THE HYDROGENOTROPHIC METHANOGENIC PATHWAY

Coenzymes and Prosthetic Groups

The biochemical reduction of CO_2 to CH_4 within the methanogenic pathway involves several coenzymes and metallocofactors that serve either as one-carbon carriers or as redox carriers in the form of cosubstrates or prosthetic groups (**Figure 1**). Most of these coenzymes were, meanwhile, also identified in other microorganisms besides methanotrophic archaea, which execute the reverse methanogenic pathway. The first methanogenic C_1-unit carrier is methanofuran (MFR), which is also used for degrading lactate to CO_2 in sulfate-reducing archaea such as *Archaeoglobus fulgidus* (75) and for formaldehyde oxidation to CO_2 by some methylotrophic bacteria (18). MFR is an amino-methyl furan tyramine derivative that has the capability to bind a C_1 unit as a formyl to its amino group (4). In methylotrophic bacteria, MFR contains a tyrosine residue instead of a tyramine, which is connected to 12–24 glutamate residues covalently attached at its end by forming amide bonds with either their α- or γ-carboxyl groups (49, 50). Tetrahydromethanopterin (H_4MPT), the second C_1 carrier of methanogenic archaea, is, as MFR, used by sulfate-reducing archaea and methylotrophic bacteria (18, 75). H_4MPT is a structural and functional analog of tetrahydrofolate (115) and acts as an equivalent C_1 carrier by binding C_1 units in the form of N^5-formyl-; N^5,N^{10}-methenyl-; N^5,N^{10}-methylene-; and N^5-methyl-. Its side chain is modified in *Methanosarcinales* by prolongation with one α-linked glutamate and in methylotrophic bacteria by omission of the phosphate and hydroxyglutarate groups (18, 20, 128). Coenzyme M (CoM-SH, 2-mercaptoethylsulfonate), the third C_1 carrier of methanogenesis, is also used in the epoxide metabolism of aerobic bacteria (3, 20, 72). CoM-SH binds a methyl group to form the thioether methyl-S-CoM.

The first redox carrier is coenzyme F_{420}. Its deazaflavin structure resembles that of flavins (FAD and FMN), but its redox potential ($F_{420}/F_{420}H_2$, $E^{\circ\prime} = -340$ mV) is similar to that of NAD(P) [$NAD(P)^+/NAD(P)H$, $E^{\circ\prime} = -320$ mV] (37). The second electron carrier is coenzyme B (CoB-SH, 7-mercaptoheptanoylthreonine phosphate), so far only discovered in methanogens and ANME. Its terminal thiol group is oxidized with CoM-SH to a heterodisulfide (CoM-S-S-CoB) (20, 80); the redox potential is $E^{\circ\prime} = -140$ mV (114).

Besides the ubiquitous cofactors FAD, molybdopterin/tungstopterin, iron-sulfur clusters, and cobalamin, prosthetic groups in methanogenic enzymes also include unusual cofactors like noncubane [4Fe-4S] clusters, the iron guanylylpyridinol (FeGP) cofactor, and coenzyme F_{430}.

Hydrogenotrophic Methanogenic Pathway

In the dominant hydrogenotrophic methanogenic pathway (**Figure 1**), CH_4 and H_2O are produced from CO_2 and molecular hydrogen (H_2), whose presence largely determines the occurrence of this process:

$$4H_2 + CO_2 \rightarrow CH_4 + 2H_2O \; \Delta G^\circ = -131 \text{ kJ/mol}.$$

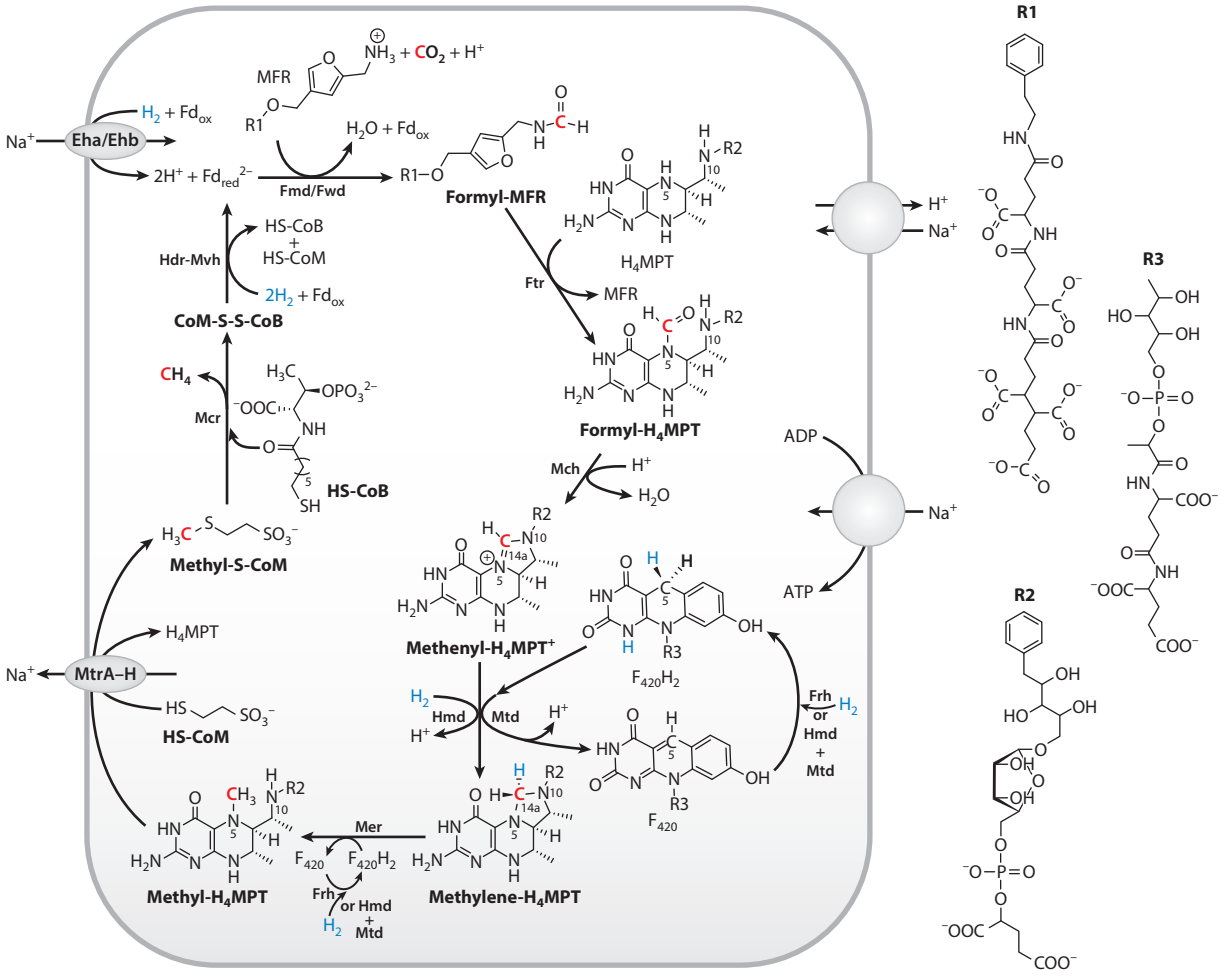

Figure 1

Overview of the hydrogenotrophic methanogenic pathway including the structure of the coenzymes. Abbreviations: HS-CoB, coenzyme B; HS-CoM, coenzyme M; Eha/Ehb, energy-converting [NiFe]-hydrogenases a and b; Fmd/Fwd, molybdopterin/tungstopterin-dependent formylmethanofuran dehydrogenase; Frh, F_{420}-reducing [NiFe]-hydrogenase; Ftr, formyltransferase; Hdr-Mvh, heterodisulfide reductase–[NiFe]-hydrogenase; H_4MPT, tetrahydromethanopterin; Hmd, H_2-forming methylene-H_4MPT dehydrogenase; Mch, methenyl-H_4MPT cyclohydrolase; Mcr, methyl–coenzyme M reductase; Mer, methylene-tetrahydromethanopterin reductase; MFR, methanofuran; Mtd, F_{420}-dependent methylene-H_4MPT dehydrogenase; Mtr, methyltransferase.

It starts with the reductive fixation of CO_2, which results in a formyl group bound to MFR (123). The formyl group is transferred to H_4MPT (11, 22), followed by a ring-closure reaction to methenyl-H_4MPT^+ (10, 21, 108). The methenyl carbon is further reduced to methylene and then to methyl via hydride transfer from $F_{420}H_2$, the reduced form of coenzyme F_{420} (61, 109). Under Ni-sufficient conditions ($Ni^{2+} > 5\ \mu M$ in the medium), $F_{420}H_2$ is regenerated by H_2 oxidation (29, 67). Under Ni-limiting conditions ($Ni^{2+} < 0.2\ \mu M$), $F_{420}H_2$ is recycled by coupling the reduction of methenyl-H_4MPT^+ by H_2 with the oxidation of the formed methylene-H_4MPT by F_{420} reduction (2). The subsequent exergonic methyl group transfer from methyl-H_4MPT to CoM-SH is coupled to Na^+-ion translocation across the cytoplasmic membrane (34). This reaction is the only

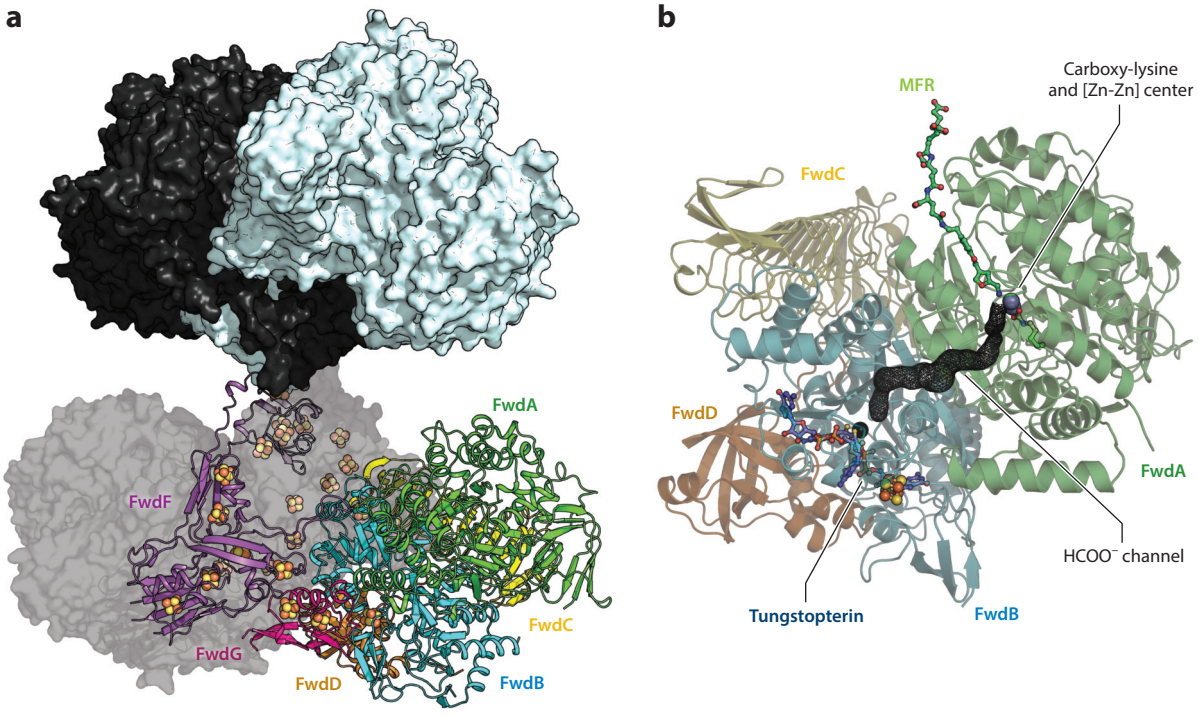

Figure 2

(*a*) Crystal structure of Fwd from *Methanothermobacter wolfeii* in the tetrameric form Fwd(ABCDFG)$_4$ (PDB: 5T61). One FwdABCDFG module is shown as a ribbon diagram and the others by surface presentation with different colors. (*b*) Catalytic mechanism (123). W, tungstopterin, Zn, carboxylysine, and MFR are shown in balls and sticks and colored in black, blue, gray, dark green, and light green, respectively. Abbreviations: Fwd, tungstopterin-dependent formylmethanofuran dehydrogenase; MFR, methanofuran; PDB, Protein Data Bank.

ion-gradient-forming process in hydrogenotrophic methanogenesis. The resulting chemiosmotic energy is essentially used to produce ATP from ADP and phosphate by Na^+ translocation (A_1A_0-ATP synthase) (33, 34). Methyl-S-CoM is finally reduced with the reducing agent CoB-SH (20) to the end product CH_4 and the heterodisulfide of coenzymes M and B (CoM-S-S-CoB) (112). Both CoM-S-S-CoB and ferredoxin are reduced by oxidizing H_2 integrated into a recently discovered energy-coupling process termed flavin-based electron bifurcation (FBEB) (46, 48, 59, 94, 114). Reduced ferredoxin drives the first endergonic CO_2 reduction reaction (59) and thus saves ATP or ion-motive energy. As a portion of reduced ferredoxin and methyl-H_4MPT is abstracted for anabolic purposes, an ion-gradient-consuming process takes a small portion of the Na^+ gradient to generate reduced ferredoxin by oxidizing H_2 (65, 110, 111, 113) (**Figure 1**).

THE ENZYME REACTION CAPTURING CO_2

The initial step in hydrogenotrophic methanogenesis is the reductive CO_2 fixation catalyzed by formylmethanofuran dehydrogenase. Two isoenzymes exist, Fmd and Fwd, carrying molybdopterin and tungstopterin as prosthetic groups, respectively (8, 52–54, 91, 92). The recent crystal structure of Fwd from *Methanothermobacter wolfeii* (123) (**Figure 2**) reveals a modular architecture,

composed of the two separated catalytic modules, formate dehydrogenase (FwdBD) and metallohydrolase (FwdA), and an electron-conducting module (FwdFG) integrated into a huge dimeric Fwd(ABCDFG)$_2$ or tetrameric Fwd(ABCDFG)$_4$ protein complex (123) (**Figure 2*a***). The central electron-conducting module is made of a dimer of two polyferredoxins carrying 16 [4Fe-4S] clusters that are connected in the *M. wolfeii* enzyme to an hourglass-like tetramer by two additional [4Fe-4S] clusters.

The inert linear CO_2 is first reduced to formate in the formate dehydrogenase module. The buried reactive center is only accessible from outside by a narrow and hydrophobic channel suitable for CO_2 and not for larger and polar compounds. The tungstopterin is reduced by a low-potential ferredoxin mediated by a series of [4Fe-4S] clusters of FwdFG. Thus, CO_2 reduction becomes exergonic ($\Delta G^{\circ\prime} = -16$ kJ/mol) (114). As the tungstopterin site is highly similar to that of bacterial formate dehydrogenases, an analogous mechanism is assumed (123).

The generated formate molecules cannot be released but are forced to migrate via a 43-Å-long, hydrophilic channel to the active site of the metallohydrolase module on which formate is conjugated with MFR (**Figure 2*b***). A mechanism was proposed in which a binuclear Zn^{2+} center and a strictly conserved aspartate act as acid/base catalysts for the amidation reaction (123). Interestingly, the formyl-MFR formation is endergonic ($\Delta G^{\circ\prime} = +16$ kJ/mol) (60, 114) but proceeds without ATP consumption, which is in contrast to the tetrahydrofolate-dependent C_1 metabolism in bacteria requiring one ATP for formate activation (16). We speculate that the high local formate concentration in the tightly closed channel shifts the equilibrium toward formyl-MFR (123). The function of 46 [4Fe-4S] clusters in the 800-kDa apparatus remains obscure. One possibility is that the four tungstopterin active sites, localized more than 200 Å apart from each other, are connected via an electronic wire that may store electrons and maintain the W(IV)/Mo(IV) state to suppress the back reaction from surplus formate in the channel to CO_2.

THE FORMYL- TO METHYL- CONVERSION AT THE THERMODYNAMIC EQUILIBRIUM

Formyl-Methanofuran: H_4MPT Formyltransferase

Formyltransferase (Ftr) catalyzes the reversible formyl-transfer reaction from formyl-MFR to H_4MPT to generate N^5-formyl-H_4MPT ($\Delta G^{\circ\prime} = -4.4$ kJ/mol) (11, 22, 104). According to crystal structures from *Methanopyrus kandleri*, *Methanosarcina barkeri*, and *A. fulgidus* Ftr (27, 71) (**Figure 3*a***), the dimeric form is essential for catalysis, but a tetrameric form conferred stability, as shown for the *M. kandleri* enzyme (104–106). The Ftr ternary complex structure reveals substrate binding sites in two neighbored clefts localized in two monomers (1). Formyl-MFR binds first, and subsequent H_4MPT binding induces conformational changes of its binding site to adjust an optimal geometry between the reacting formyl carbon of the furanamide and N5 of the pterin groups, coinciding at the buried dimer interface. The metal-free transamidation reaction is started by a nucleophilic attack of N5 on the formyl carbon, thus forming a tetrahedral anion intermediate that is stabilized by the strictly conserved Glu245 acting as an acid/base catalyst (1) (**Figure 3*b***).

Methenyl-H_4MPT Cyclohydrolase

Methenyl-H_4MPT cyclohydrolase (Mch) catalyzes a condensation reaction of formyl-H_4MPT to methenyl-H_4MPT$^+$ ($\Delta G^{\circ\prime} = -4.6$ kJ/mol) (10, 21, 108). The X-ray structure of Mch revealed a homotrimeric complex (36) (**Figure 3*c***) with a deep active site cleft placed between the two

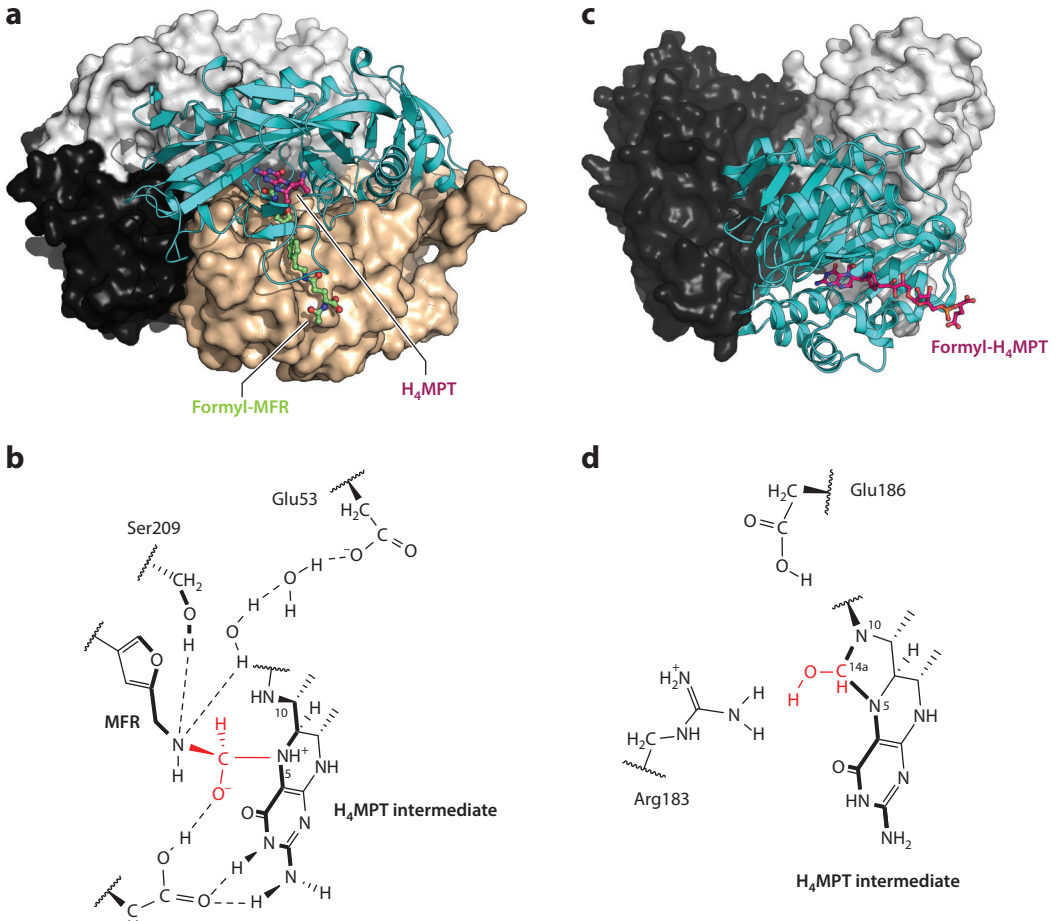

Figure 3

Ftr from *Methanopyrus kandleri* and Mch from *Archaeoglobus fulgidus*. (*a*) Crystal structure of Ftr complexed with formyl-MFR and H_4MPT (shown as *balls and sticks*) in the tetrameric form (PDB: 2FHJ). One monomer is shown as a ribbon diagram and the others by surface presentation with different colors. (*b*) Catalytic mechanism. The nucleophilic attack of N5 of H_4MPT on the formamide-C of formyl-MFR is facilitated by Glu245, which enhances the electrophilicity of the latter and may stabilize the tetrahedral oxyanion intermediate by protonation. Then, formyl-H_4MPT is formed (1). Ser209 and solvent molecules linked with Glu53 are presumably involved in the protonation/deprotonation of the amine group. (*c*) Structure of trimeric Mch bound with formyl-H_4MPT (PDB: 4GVS). One monomer is shown as a ribbon diagram and the others by surface presentation with different colors. (*d*) Catalytic mechanism. The N10 of formyl-H_4MPT nucleophilically attacks the formyl carbon forming a tetrahedral C14a hydroxyl intermediate (119). The key catalytic player is Glu186, which protonates the thereby generated anionic tetrahedral intermediate, accepts a proton from the formed N10 ammonium ion, and facilitates dehydration by protonating the C14a hydroxyl group. Arg183 modulates the acid/base capabilities of Glu186. Abbreviations: Ftr, formyltransferase; H_4MPT, tetrahydromethanopterin; Mch, methenyl-H_4MPT cyclohydrolase; MFR, methanofuran; PDB, Protein Data Bank.

domains of each monomer. According to the Mch-formyl-H_4MPT complex structure, the pterin and phenyl groups are oriented nearly perpendicularly, which optimally positions the reacting N10 and formyl carbon relative to each other for a nucleophilic addition (119) (**Figure 3*d***). The conserved Glu186 acts as an acid/base catalyst. The crucial roles of Glu186 and the neighbored Arg183 have been substantiated by site-directed mutagenesis.

Methylene-H_4MPT Dehydrogenases

The hydrogenotrophic methanogenic pathway employs two types of methylene-H_4MPT dehydrogenases (97, 109, 132) catalyzing the reversible reduction of methenyl-H_4MPT^+ to methylene-H_4MPT by hydride transfer. The F_{420}-dependent methylene-H_4MPT dehydrogenase (Mtd) uses $F_{420}H_2$ as an electron donor ($\Delta G^{\circ\prime} = +5.5$ kJ/mol) (109) and is structurally characterized as a homohexameric protein complex (15, 38) (**Figure 4*a***). The crystal structure of the Mtd–methenyl-H_4MPT^+–$F_{420}H_2$ complex indicates that the fixed interdomain crevice imposes constraints on the deformable multicyclic substrate rings (15). As a consequence, the phenyl-imidazolidine-tetrahydropyrazine rings of methenyl-H_4MPT^+ and the deazaisoalloxazine ring of $F_{420}H_2$ are arranged roughly parallel to each other in a manner to avoid collisions and, in parallel, to create a favorable hydride transfer geometry prior to the reaction (**Figure 4*b***). The compressed conformation, documented as a distance of 2.7 Å between the hydride-transferring C14a and C5 atoms, enhances the catalytic activity perhaps via a tunneling effect, as reported for NADP-dependent methylene-H_4MPT dehydrogenase (55) and flavoproteins (43).

H_2-forming methylene-H_4MPT dehydrogenase (Hmd), also termed [Fe]-hydrogenase (**Figure 4*c***), uses H_2 as an electron donor ($\Delta G^{\circ\prime} = -5.5$ kJ/mol) (51, 62, 68, 85, 97, 100–103, 132) and is therefore the only enzyme in nature that directly uses a hydride from H_2 for hydride transfer reactions. H_2 activation/cleavage in the homodimeric enzyme is primarily achieved by a unique prosthetic group, the FeGP cofactor (97) (**Figure 4*d***). Mechanistically, the closure of the intersubunit active site cleft upon methenyl-H_4MPT^+ binding results in an expulsion of the H_2O molecule ligated to the Fe(II) center (51, 57, 121) (**Figure 4*c,d***). H_2 occupies the empty Fe coordination site and is heterolytically cleaved. The resulting hydride is transferred to the C14a of methenyl-H_4MPT^+. Recent mimic compounds have not only underpinned the 2-OH group as a base (96) but also offered perspectives for biotechnological applications (81, 96).

F_{420}-Dependent Methylene-H_4MPT Reductase

Methylene-tetrahydromethanopterin reductase (Mer) catalyzes a reversible hydride transfer from $F_{420}H_2$ to methylene-H_4MPT to generate F_{420} and methyl-H_4MPT ($\Delta G^{\circ\prime} = -6.2$ kJ/mol) (70, 104, 114). The crystal structures of Mer from *M. kandleri*, *Methanothermobacter marburgensis*, and *M. barkeri* (7, 107) reveal homodimeric and homotetrameric forms with a triose-phosphate isomerase $\alpha_8\beta_8$ barrel fold of the monomer as reported for some flavin-dependent oxidoreductases (6). The electron donor F_{420} is bound to the polypeptide in a pronounced butterfly conformation at the C-terminal side of the central β sheet. Interestingly, the central pyridine ring with the hydride-transferring C5 is kept outside the plane by a nonprolyl *cis*-peptide between Gly61 and Val62, where Val62 acts as a backstop of F_{420} at its *re*-face. Methylene-H_4MPT binding at the *si*-face of F_{420} is not established yet due to the lack of structural data. However, similar general principles of hydride transfer as described for Mtd may also be valid for Mer. Heterologous production of Mer failed for a long time, probably because of the nonprolyl *cis*-peptide bond; recently, however, it succeeded for the *Methanocaldococcus jannaschii* enzyme (73).

F_{420}-Reducing [NiFe]-Hydrogenase

F_{420}-reducing [NiFe]-hydrogenase (Frh) is a group 3 [NiFe]-hydrogenase and catalyzes the reversible hydrogenation of F_{420} using electrons from H_2 ($\Delta G^{\circ\prime} = -10$ kJ/mol) (29). Both cryo–electron microscopy and crystal structures revealed a huge protein complex with a molecular mass of 1.25 MDa made up of an FrhAGB protomer assembled via a tight dimer to a dodecameric

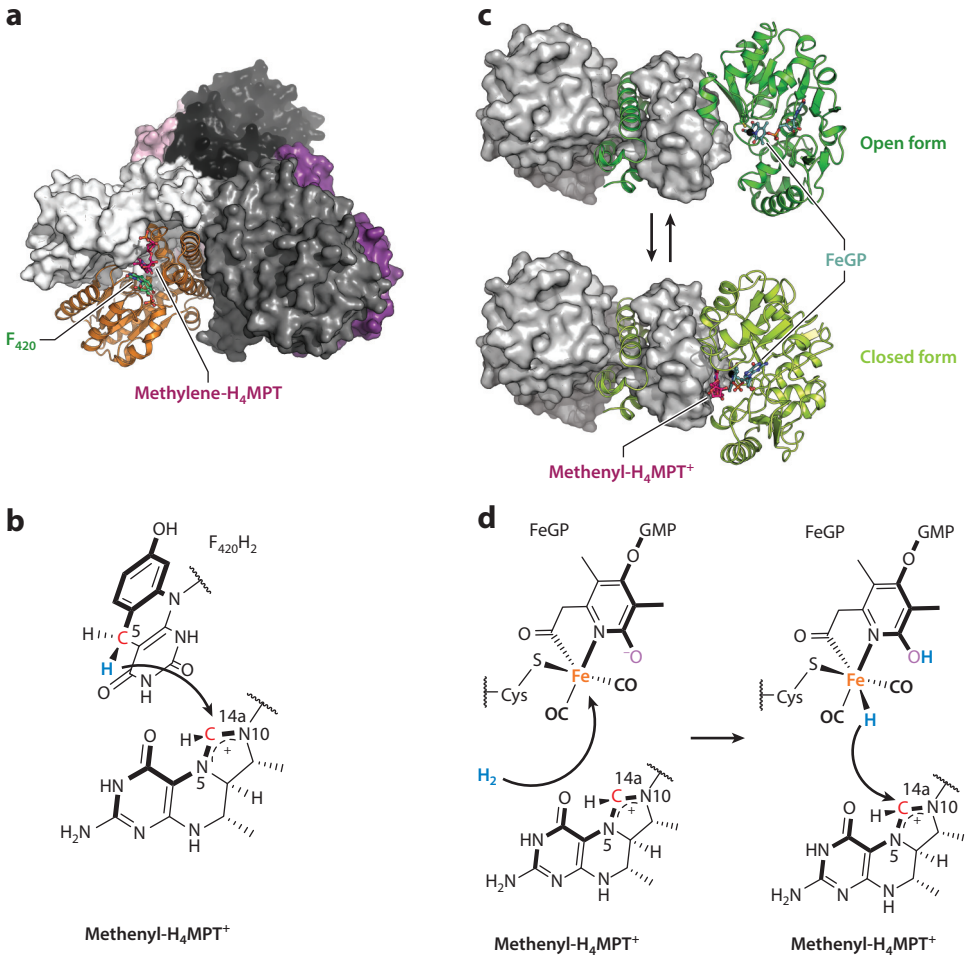

Figure 4

Mtd from *Methanopyrus kandleri* and Hmd from *Methanococcus aeolicus*. (*a*) Homohexameric structure of Mtd in complex with methenyl-H_4MPT^+ and $F_{420}H_2$ (PDB: 3IQE). One monomer is shown as a ribbon diagram and the others by surface presentation with different colors. The active site crevice is located between two domains of one subunit covered by a loop from another subunit. (*b*) Catalytic mechanism. The *pro-S* hydride on C5 of $F_{420}H_2$ is directly transferred to the *pro-R* position of C14a of methenyl-H_4MPT^+ (15). (*c*) Homodimeric Hmd structures in the open (PDB: 6HAC) and closed (PDB: 6HAV) forms, both with the FeGP cofactor. One monomer is shown as a ribbon diagram and the other by surface presentation. The closed form is induced by binding of methenyl-H_4MPT^+. (*d*) Catalytic mechanism. The FeGP cofactor contains an Fe(II) center ligated with one acyl-methyl substituent and one N of guanylylpyridinol, two CO, one cysteine sulfur, and one H_2O (not shown here). The catalytic cycle starts with a domain closure and H_2O ligand removal. H_2 binds to the resulting 5-coordinated Fe(II) and becomes heterolytically cleaved. The proton is abstracted by the deprotonated 2-OH group of the FeGP cofactor, and the hydride of the postulated Fe-H intermediate is transferred to the C14a of methenyl-H_4MPT^+ (57). Abbreviations: FeGP, iron guanylylpyridinol cofactor; H_4MPT, tetrahydromethanopterin; Hmd, H_2-forming methylene-H_4MPT dehydrogenase; Mtd, F_{420}-dependent methylene-H_4MPT dehydrogenase; PDB, Protein Data Bank.

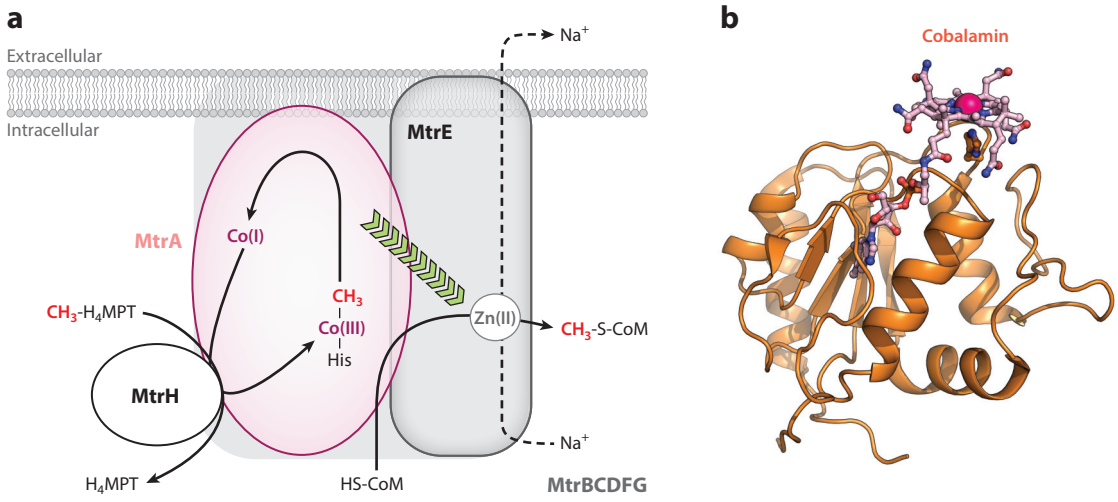

Figure 5

The MtrA–H complex. (*a*) Schematic representation of the structure and catalytic mechanism (34). MtrB–G constitute the membrane part, MtrH is weakly attached to the membrane part, and the soluble MtrA domain carries the cobalamin cofactor (*pink*). (*b*) Structure of the MtrA cytoplasmic homolog from *Methanothermus fervidus* (PDB: 5LAA). The prosthetic group, cobalamin (*ball and stick*), sits at the C-terminal end of the parallel β sheet in an exposed manner. Abbreviations: HS-CoM, coenzyme M; H_4MPT, tetrahydromethanopterin; Mtr, methyltransferase; PDB, Protein Data Bank.

quaternary structure (74, 120). The internal space of the hollow cube is connected to bulk solvent by pores with a diameter of ca. 8 Å. No convincing hypothesis exists concerning the purpose of the enormous size of the Frh complex and its voluminous cavity. FrhA contains the canonical [NiFe]-center for H_2 cleavage, and FrhG hosts three [4Fe-4S] clusters for single electron transfer to FrhB that harbors a [4Fe-4S] cluster and an FAD required for the hydride transfer to F_{420}.

SODIUM-ION TRANSLOCATING METHYL-TRANSFER PROCESS

Na^+-Ion Translocating Methyl-H_4MPT: Coenzyme-M Methyltransferase

Methyl-H_4MPT: coenzyme M methyltransferase (MtrA–H) carrying the cofactor 5-hydroxybenzimidazolyl cobamide, a cobalamin derivative (34), catalyzes the methyl transfer from methyl-H_4MPT to CoM-SH ($\Delta G^{\circ\prime} = -30$ kJ/mol) coupled with Na^+ translocation. This reaction is a two-step process (30, 31, 40, 41, 127) (**Figure 5*a***): transfer of the methyl group (*a*) from methyl-H_4MPT to Co(I) ($\Delta G^{\circ\prime} = -15$ kJ/mol) and (*b*) from methyl-Co(III) to CoM-SH ($\Delta G^{\circ\prime} = -15$ kJ/mol) (34). The demethylation from methyl-Co(III) is Na^+ dependent, which suggests a connection of the second step with Na^+-ion translocation across the cytoplasmic membrane (31, 127). The membrane protein has been found as a homotrimeric Mtr(ABCDEFGH)$_3$ complex (118). MtrE hosts a potential Zn^{2+} well suited for CoM-SH methylation and an aspartate in a highly conserved segment of the membrane-spanning region probably involved in Na^+ translocation (34). MtrH contains the site of methyl-H_4MPT demethylation and MtrA, the site of cobalamin cofactor binding.

Structure of the MtrA Subunit

Structural information about the MtrA–H complex is only available for MtrA from *M. jannaschii* and the cytoplasmic MtrA homolog from *Methanothermus fervidus* (**Figure 5*b***). MtrA adopts a

Rossmann-like open α/β fold (23), but, most remarkably, the cobalamin in MtrA binds to the opposite side of the central β sheet compared to all other cobalamin-dependent methyltransferases adopting the same overall fold (122). Nevertheless, MtrA contains the His-Glu-proton-donor triad at the lower distal Co(III) binding site, a common trait of these methyltransferases despite their different positions. In MtrA, the His-Glu-proton-donor triad is connected to a conserved elongated segment, which only loosely attaches to the MtrA core. Possible conformational changes might be induced by the different position of the His imidazolium in the Co(III)-His on and Co(I)-His off configurations (122). On this basis, we speculate that the cytoplasmic part of MtrA attached to MtrH swings as a consequence of methyl-Co(III) formation to the CoM-SH binding site localized at MtrE. Then, the chemical energy of the methyl-Co(III) demethylation reaction is transformed via the elongated segment of MtrA into mechanical energy of the membrane-spanning region of MtrE to open a passage for Na^+ (34) (**Figure 5*a***).

CH_4-PRODUCING REACTION

Methyl–Coenzyme M Reductase

Methyl–coenzyme M reductase (Mcr) catalyzes the CH_4-forming reaction in all variants of the methanogenic pathway (112) and the first CH_4-activating reaction in the anaerobic CH_4 oxidation pathway of ANME (42, 63, 99). The reversibility of the Mcr reaction was experimentally demonstrated using the enzyme from *M. marburgensis* (90). Recently, evidence has been provided that Mcr homologs catalyze the anaerobic oxidation of butane, propane, and ethane (17, 64).

The chemically intricate reductive thioether cleavage of methyl-S-CoM to CH_4 is energetically far away from the conventional hydride transfer chemistry described above and has no direct mimic in organic chemistry. The enormous synthetic challenge forced evolution to develop, exclusively for the Mcr reaction, a new prosthetic group, the coenzyme F_{430} (28, 66, 84), and a new electron donor, CoB-SH, including the biosynthesis machinery behind. F_{430} is apparently designed for reaching a highly reactive but just manageable Ni(I) oxidation state $\{E^{o\prime}[\text{Ni(I)/Ni(II)}] < -600\ \text{mV}\}$ to reductively attack the inert C-S bond (112). The instability of the Ni(I) state, which is already oxidized to Ni(II) at a too-low cellular redox potential, is a serious handicap for the organism. Therefore, a sophisticated machinery to regenerate Ni(I) with ATP consumption exists (86). For the same reason, Mcr from methanogenic archaea is purified as an inactive MCR_{silent} [EPR-silent Ni(II) state] or MCR_{ox1} state [exhibiting EPR_{ox1} Ni(III) signal] (35, 87), which can be activated to the MCR_{red1} state [EPR_{red1} Ni(I) signal] afterward by enzymological activation methods (35, 86, 87, 131). Only the MCR_{ox1} state can also be activated by a chemical method. However, even in strictly anaerobic media, the MCR_{red1} form is steadily converted to the MCR_{silent} state (35).

Mcr has been structurally characterized at high resolution from several organisms, albeit solely in inactive Ni(II) states. Architecturally, Mcr is constructed as an $(\alpha\beta\gamma)_2$ heterohexameric complex (**Figure 6*a***) with F_{430} (**Figure 6*b***) deeply embedded inside the protein matrix and only accessible from bulk solvent by a 30-Å-long, narrow channel. In the $MCR_{ox1\text{-}silent}$ [EPR-silent Ni(II) state] structure, CoM-SH is bound in front of F_{430} with its sulfur coordinated to the upper axial Ni ligation site. CoB-SH is accommodated in the channel with its threonine-phosphate group plugging the entrance and the heptanoyl thiol group pointing toward the front side of F_{430}. In the MCR_{silent} structure, the CoM-S-S-CoB heterodisulfide is covalently bound to the Ni(II) of F_{430} by the sulfonate-oxygen of the coenzyme M moiety (26).

Catalytic Mechanism

Two major types of catalytic mechanisms, controversially discussed in the past, were proposed for the Mcr reaction. The key difference between them is how Ni(I) attacks methyl-S-CoM

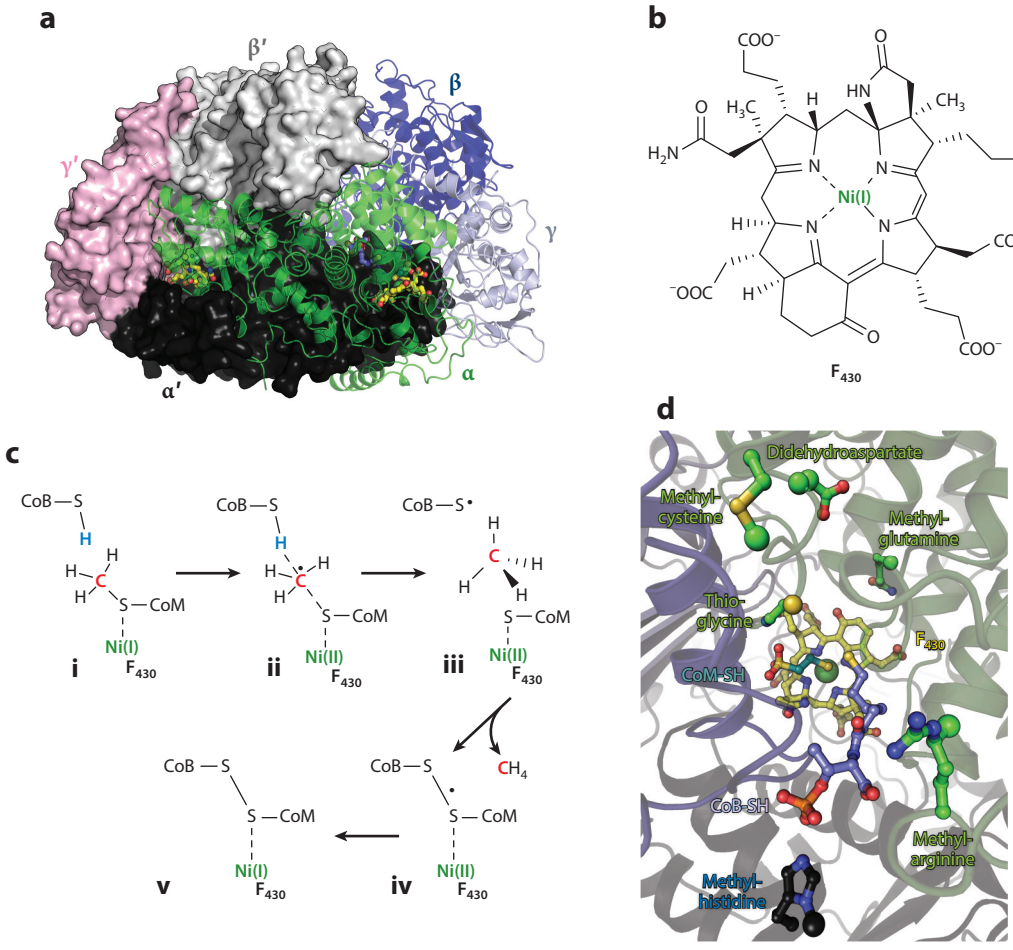

Figure 6

Structure and catalytic mechanism of Mcr. (*a*) The crystal structure of Mcr from *Methanothermobacter marburgensis*. The heterohexamer contains two active sites; each of them contains F_{430} (*yellow*), CoM-SH (*green-blue*), and CoB-SH (*dark blue*) (PDB: 5A0Y). One αβγ unit of the Mcr heterohexamer $(\alpha\beta\gamma)_2$ is shown as a ribbon diagram and the other by surface presentation, in which the α, β, and γ subunits are differentiated by colors. (*b*) Chemical structure of F_{430}. (*c*) The methyl radical mechanism (82, 112, 129, 130). (*i*) The S-C bond of methyl-S-CoM is attacked by the reactive Ni(I), forming (*ii*) a planar methyl radical and a Ni(II)-S-CoM intermediate. (*iii*) The methyl radical captures the H atom from neighbored CoB-SH, thereby producing CH_4 and a CoB thiyl radical. (*iv*) CH_4 is released, and a heterodisulfide thiyl radical is formed. (*v*) One electron of the latter is transferred to Ni(II) for regenerating Ni(I). (*d*) Modified amino acid residues at the active site (26, 93, 124). A thioglycine, 1-*N*-methyl-histidine, *S*-methyl-cysteine, 5-methyl-arginine, 2-methyl-glutamine, and didehydroaspartate are found in *M. marburgensis* Mcr (highlighted by a *larger ball*). In addition, 6- and 7-hydroxytryptophane were found in *Methanotorris formicicus* Mcr and an ANME-1 archaeon MCR, respectively (99, 126). Abbreviations: ANME, anaerobic methanotrophic archaea; CoB-SH, coenzyme B; CoM-SH, coenzyme M; CoB-S-S-CoM, heterodisulfide of CoM-SH and CoB-SH; Mcr, methyl–coenzyme M reductase; PDB, Protein Data Bank.

(112). In the first scenario, Ni(I) nucleophilically attacks the methyl group of methyl-S-CoM, forming a transient methyl-Ni(III) intermediate that breaks into CH_4 and a coenzyme M thiyl radical (26). The second scenario starts with an attack of Ni(I) onto the sulfur of methyl-S-CoM, resulting in a transient methyl radical and a CoM-S-Ni(II) intermediate (82) (**Figure 6*c***). Recent biochemical and spectroscopic analyses detected the latter intermediate, which strongly supports

the methyl-radical mechanism (95, 130). EPR and UV/visible spectroscopic data showed that only one of the two active sites of Mcr is active, suggesting cooperativity between them similar to that in an opposed piston engine (32, 116). The observed large conformational changes of CoB-SH toward Ni and porphinoid ring distortions (24) in one active site might be driven by exergonic events at the counteractive site.

Posttranslational Modifications

Mcr contains several posttranslational modifications in the α subunit adjacent to the active site that might affect the enzymatic activity (26, 58, 93, 124, 126) (**Figure 6*d***). Recently, genes for methyltransferases responsible for the methyl-arginine modification (19) and the methyl-cysteine modification (76), and for a thioglycine-forming enzyme (77) were deleted, indicating no essential influence on the Mcr reaction but not excluding an effect under special environmental conditions of life. The recent successful production of Mcr from *Methanothermococcus okinawensis* in the mesophilic *Methanococcus maripaludis* allowed site-directed mutagenesis experiments for more profound mechanistic studies (69).

ELECTRON-BIFURCATING REACTION FOR FERREDOXIN REDUCTION

Heterodisulfide Reductase/Hydrogenase Complex

The regeneration of the C_1 carrier CoM-SH and the reducing agent CoB-SH from CoM-S-S-CoB is used to fuel the endergonic ferredoxin reduction via an FBEB mechanism (12–14, 59). The process is initiated by H_2 oxidation, and the two electrons ($E^{\circ\prime} = -414$ mV) are transferred to the bifurcating flavin, which is endowed with two single-electron redox potentials, $FADH^-$/FADH• and FADH•/FAD, of different energy. Then, the electrons of $FADH^-$ are donated toward two directions (125): The first high-potential electron is transferred to the high-potential electron acceptor, CoM-S-S-CoB ($E^{\circ\prime} = -140$ mV), and the second low-potential electron to the low-potential electron acceptor ferredoxin ($E^{\circ\prime} \approx -500$ mV). These reactions run twice. The FBEB process is catalyzed by the HdrABC–MvhAGD complex (44–48, 94), whose crystal structure from *Methanothermococcus thermolithotrophicus* was recently elucidated (125) (**Figure 7*a***). Both hexameric protomers of the heterododecameric protein complex are composed of an HdrA core (hosting the central bifurcating FAD and 6 [4Fe-4S] clusters) and three arms branching off; each arm catalyzes a redox process at its end. The electron-donating arm consists of MvhA ([NiFe] center) and MvhG (three [4Fe-4S] clusters), which corresponds to a [NiFe]-hydrogenase module and MvhD ([2Fe-2S] cluster), the adaptor to HdrA. The high-potential electron-accepting arm consists of HdrB (two noncubane [4Fe-4S clusters]), the site of CoM-S-S-CoB reduction and HdrC (two [4Fe-4S] clusters), the adaptor to HdrA. The low-potential electron-accepting arm is postulated to extend to the periphery of the ferredoxin-like domain of HdrA, the proposed binding site for exogenous ferredoxin. The first static picture of the HdrABC–MvhAGD complex provides an interrupted electron transfer chain (distance longer than 15 Å between electron carriers) between the [NiFe]-center and FAD as well as between FAD and the ferredoxin-binding domain, whereas electrons can flow from FAD to the noncubane [4Fe-4S] clusters. How conduction/interruption between FAD and the three distant redox processes and their coordination is achieved during FBEB is not understood yet. Although the structural data offer several plausible scenarios, the N-terminal domain of HdrA appears to play a key role. Its [4Fe-4S] cluster may electronically link FAD with the H_2-cleaving [NiFe] center by a swinging process and with the [4Fe-4S] clusters of the ferredoxin-binding domain conformationally rearranged upon ferredoxin binding.

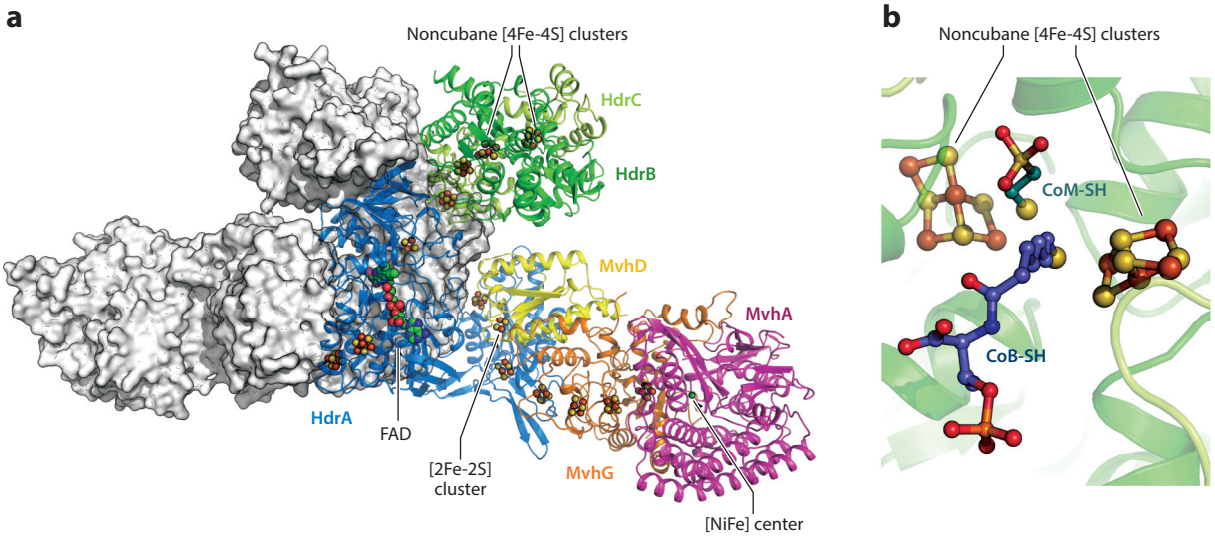

Figure 7

The HdrABC–MvhAGD complex. (*a*) Overall dimeric structure of *Methanothermococcus thermolithotrophicus* enzyme (PDB: 5ODC). One HdrABC–MvhAGD unit is shown as a ribbon diagram and the other by surface presentation, in which the subunits are differentiated by colors. The cofactors are shown by balls and sticks. (*b*) The CoM-S-S-CoB reduction site. Two novel noncubane [4Fe-4S] clusters clamp the substrate between the two closest Fe. The two-electron reduction of the disulfide is achieved by a one-electron oxidation of each noncubane [4Fe-4S] cluster. Abbreviations: CoB-SH, coenzyme B; CoM-SH, coenzyme M; Hdr, heterodisulfide reductase; Mvh, [NiFe]-hydrogenase; PDB, Protein Data Bank.

Noncubane [4Fe-4S] Cluster

The CoM-S-S-CoB reduction on HdrB is accomplished by a unique catalytic principle (125). HdrB harbors two identical noncubane [4Fe-4S] clusters each composed of a [3Fe-4S]-[2Fe-2S] unit that shares one Fe and one inorganic sulfur. Remarkably, one of the bridging sulfurs originates from a cysteine. CoM-S-S-CoB settles between the closest Fe of two facing clusters, as deduced from the trapped ternary complex (**Figure 7*b***). Disulfide is homolytically cleaved, and the coenzyme M and B sulfurs covalently bind to the noncubane [4Fe-4S] clusters. The thereby oxidized noncubane clusters are reduced one-by-one by two one-electron steps by which CoB-SH and CoM-SH are successively released. Thus, both noncubane clusters together operate like a flavin. Time-dependent crystal-soaking experiments revealed that CoB-SH is released first upon one-electron reduction of the noncubane [4Fe-4S] cluster and CoM-SH second (125). This type of disulfide reduction is presumably widespread in biochemistry because the noncubane [4Fe-4S] clusters are bound to the CCG sequence motif, $CX_{31–39}CCX_{35–36}CXXC$, which is conserved in many bacteria and archaea (39, 83).

CONCLUSIONS AND FUTURE PERSPECTIVES

In the most recent decades, all the cytosolic enzymes of hydrogenotrophic methanogenesis, mostly in complex with their substrates/products, were structurally characterized and a rather detailed picture of the catalytic process was established, involving biochemical, kinetic, and site-directed mutagenesis data. For gaining deeper insights into the catalytic mechanism, current studies have to be completed and novel biophysical methods including time-resolved techniques have to be tested out on the complex reactions of methanogenesis. In particular, cryo–electron microscopy,

substantially advanced in recent years, might be applied for structure determination of the energy-conserving membrane complex Mtr, for exploring enzymes like Mcr in the active state [so far it has only been characterized in an inactive state (26, 98, 112)], and for identifying distinct conformational states in the catalytic cycle of enzymes like the HdrABC–MvhAGD complex (125). A complete understanding of methanogenic energy metabolism, in addition, requires the identification and characterization of enzymes recruited for the biosynthesis of all coenzymes and prosthetic groups. In parallel, strain characterization, development of basic genetic tools (78), and regulation studies on enzyme expression in various methanogenic organisms, e.g., in dependency of metals, in particular of Ni^{2+}, have to be continued (2). Biotechnological applications of hydrogenotrophic methanogenesis are related to individual enzymes, e.g., [Fe]-hydrogenase (56), and also to the entire pathway (9, 25).

DISCLOSURE STATEMENT

The authors are not aware of any affiliations, memberships, funding, or financial holdings that might be perceived as affecting the objectivity of this review.

ACKNOWLEDGMENTS

This work was supported by grants from the Max Planck Society (to S.S., T.W., and U.E.) and Deutsche Forschungsgemeinschaft (SH 87/1-1, to S.S.).

LITERATURE CITED

1. Acharya P, Warkentin E, Ermler U, Thauer RK, Shima S. 2006. The structure of formylmethanofuran: tetrahydromethanopterin formyltransferase in complex with its coenzymes. *J. Mol. Biol.* 357:870–79
2. Afting C, Hochheimer A, Thauer RK. 1998. Function of H_2-forming methylenetetrahydromethanopterin dehydrogenase from *Methanobacterium thermoautotrophicum* in coenzyme F_{420} reduction with H_2. *Arch. Microbiol.* 169:206–10
3. Allen JR, Clark DD, Krum JG, Ensign SA. 1999. A role for coenzyme M (2-mercaptoethanesulfonic acid) in a bacterial pathway of aliphatic epoxide carboxylation. *PNAS* 96:8432–37
4. Allen KD, White RH. 2014. Identification of structurally diverse methanofuran coenzymes in methanococcales that are both N-formylated and N-acetylated. *Biochemistry* 53:6199–210
5. Archer D, Buffett B, Brovkin V. 2009. Ocean methane hydrates as a slow tipping point in the global carbon cycle. *PNAS* 106:20596–601
6. Aufhammer SW, Warkentin E, Berk H, Shima S, Thauer RK, Ermler U. 2004. Coenzyme binding in F_{420}-dependent secondary alcohol dehydrogenase, a member of the bacterial luciferase family. *Structure* 12:361–70
7. Aufhammer SW, Warkentin E, Ermler U, Hagemeier CH, Thauer RK, Shima S. 2005. Crystal structure of methylenetetrahydromethanopterin reductase (Mer) in complex with coenzyme F_{420}: architecture of the F_{420}/FMN binding site of enzymes within the nonprolyl *cis*-peptide containing bacterial luciferase family. *Protein Sci.* 14:1840–49
8. Bertram PA, Karrasch M, Schmitz RA, Böcher R, Albracht SPJ, Thauer RK. 1994. Formylmethanofuran dehydrogenases from methanogenic Archaea: substrate specificity, EPR properties and reversible inactivation by cyanide of the molybdenum or tungsten iron-sulfur proteins. *Eur. J. Biochem.* 220:477–84
9. Blasco-Gómez R, Batlle-Vilanova P, Villano M, Balaguer MD, Colprim J, Puig S. 2017. On the edge of research and technological application: a critical review of electromethanogenesis. *Int. J. Mol. Sci.* 18:E874. **https://doi.org/10.3390/ijms18040874**
10. Breitung J, Schmitz RA, Stetter KO, Thauer RK. 1991. N^5,N^{10}-Methenyltetrahydromethanopterin cyclohydrolase from the extreme thermophile *Methanopyrus kandleri*: increase of catalytic efficiency (k_{cat}/K_M) and thermostability in the presence of salts. *Archiv. Microbiol.* 156:517–24

11. Breitung J, Thauer RK. 1990. Formylmethanofuran: tetrahydromethanopterin formyltransferase from *Methanosarcina barkeri*; identification of N^5-formyltetrahydromethanopterin as the product. *FEBS Lett.* 275:226–30
12. Buckel W, Thauer RK. 2013. Energy conservation via electron bifurcating ferredoxin reduction and proton/Na^+ translocating ferredoxin oxidation. *Biochim. Biophys. Acta Bioenerg.* 1827:94–113
13. Buckel W, Thauer RK. 2018. Flavin-based electron bifurcation, a new mechanism of biological energy coupling. *Chem. Rev.* 118:3862–86
14. Buckel W, Thauer RK. 2018. Flavin-based electron bifurcation, ferredoxin, flavodoxin, and anaerobic respiration with protons (Ech) or NAD^+ (Rnf) as electron acceptors: a historical review. *Front. Microbiol.* 9:401
15. Ceh K, Demmer U, Warkentin E, Moll J, Thauer RK, et al. 2009. Structural basis of the hydride transfer mechanism in F_{420}-dependent methylenetetrahydromethanopterin dehydrogenase. *Biochemistry* 48:10098–105
16. Celeste LR, Chai GQ, Bielak M, Minor W, Lovelace LL, Lebioda L. 2012. Mechanism of N^{10}-formyltetrahydrofolate synthetase derived from complexes with intermediates and inhibitors. *Protein Sci.* 21:219–28
17. Chen SC, Musat N, Lechtenfeld OJ, Paschke H, Schmidt M, et al. 2019. Anaerobic oxidation of ethane by archaea from a marine hydrocarbon seep. *Nature* 568:108–11
18. Chistoserdova L, Vorholt JA, Thauer RK, Lidstrom ME. 1998. C_1 transfer enzymes and coenzymes linking methylotrophic Bacteria and methanogenic Archaea. *Science* 281:99–102
19. Deobald D, Adrian L, Schöne C, Rother M, Layer G. 2018. Identification of a unique radical SAM methyltransferase required for the sp^3-C-methylation of an arginine residue of methyl-coenzyme M reductase. *Sci. Rep.* 8:7404
20. Dimarco AA, Bobik TA, Wolfe RS. 1990. Unusual coenzymes of methanogenesis. *Annu. Rev. Biochem.* 59:355–94
21. Dimarco AA, Donnelly MI, Wolfe RS. 1986. Purification and properties of the 5,10-methenyltetrahydromethanopterin cyclohydrolase from *Methanobacterium thermoautotrophicum*. *J. Bacteriol.* 168:1372–77
22. Donnelly MI, Wolfe RS. 1986. The role of formylmethanofuran:tetrahydromethanopterin formyltransferase in methanogenesis from carbon-dioxide. *J. Biol. Chem.* 261:16653–59
23. Drennan CL, Huang S, Drummond JT, Matthews RG, Ludwig ML. 1994. How a protein binds B_{12}: a 3.0 Å X-ray structure of B_{12}-binding domains of methionine synthase. *Science* 266:1669–74
24. Ebner S, Jaun B, Goenrich M, Thauer RK, Harmer J. 2010. Binding of coenzyme B induces a major conformational change in the active site of methyl-coenzyme M reductase. *J. Am. Chem. Soc.* 132:567–75
25. Enzmann F, Mayer F, Rother M, Holtmann D. 2018. Methanogens: biochemical background and biotechnological applications. *AMB Expr.* 8:1. **https://doi.org/10.1186/s13568-017-0531-x**
26. Ermler U, Grabarse W, Shima S, Goubeaud M, Thauer RK. 1997. Crystal structure of methyl coenzyme M reductase: the key enzyme of biological methane formation. *Science* 278:1457–62
27. Ermler U, Merckel MC, Thauer RK, Shima S. 1997. Formylmethanofuran: tetrahydromethanopterin formyltransferase from *Methanopyrus kandleri*—new insights into salt-dependence and thermostability. *Structure* 5:635–46
28. Fässler A, Kobelt A, Pfaltz A, Eschenmoser A, Bladon C, et al. 1985. Factor F_{430} from methanogenic bacteria: absolute-configuration. *Helv. Chim. Acta* 68:2287–98
29. Fox JA, Livingston DJ, Orme-Johnson WH, Walsh CT. 1987. 8-Hydroxy-5-deazaflavin-reducing hydrogenase from *Methanobacterium thermoautotrophicum*: 1. purification and characterization. *Biochemistry* 26:4219–27
30. Gärtner P, Ecker A, Fischer R, Linder D, Fuchs G, Thauer RK. 1993. Purification and properties of N^5-methyltetrahydromethanopterin:coenzyme M methyltransferase from *Methanobacterium thermoautotrophicum*. *Eur. J. Biochem.* 213:537–45
31. Gärtner P, Weiss DS, Harms U, Thauer RK. 1994. N^5-methyltetrahydromethanopterin:coenzyme M methyltransferase from *Methanobacterium thermoautotrophicum*: catalytic mechanism and sodium ion dependence. *Eur. J. Biochem.* 226:465–72

32. Goenrich M, Duin EC, Mahlert F, Thauer RK. 2005. Temperature dependence of methyl-coenzyme M reductase activity and of the formation of the methyl-coenzyme M reductase red2 state induced by coenzyme B. *J. Biol. Inorg. Chem.* 10:333–42
33. Gottschalk G, Blaut M. 1990. Generation of proton and sodium motive forces in methanogenic bacteria. *Biochim. Biophys. Acta Bioenerg.* 1018:263–66
34. Gottschalk G, Thauer RK. 2001. The Na^+-translocating methyltransferase complex from methanogenic archaea. *Biochim. Biophys. Acta Bioenerg.* 1505:28–36
35. Goubeaud M, Schreiner G, Thauer RK. 1997. Purified methyl-coenzyme-M reductase is activated when the enzyme-bound coenzyme F430 is reduced to the nickel(I) oxidation state by titanium(III) citrate. *Eur. J. Biochem.* 243:110–14
36. Grabarse W, Vaupel M, Vorholt JA, Shima S, Thauer RK, et al. 1999. The crystal structure of methenyltetrahydromethanopterin cyclohydrolase from the hyperthermophilic archaeon *Methanopyrus kandleri*. *Struct. Fold. Des.* 7:1257–68
37. Greening C, Ahmed FH, Mohamed AE, Lee BM, Pandey G, et al. 2016. Physiology, biochemistry, and applications of F_{420}- and F_o-dependent redox reactions. *Microbiol. Mol. Biol. Rev.* 80:451–93
38. Hagemeier CH, Shima S, Thauer RK, Bourenkov G, Bartunik HD, Ermler U. 2003. Coenzyme F_{420}-dependent methylenetetrahydromethanopterin dehydrogenase (Mtd) from *Methanopyrus kandleri*: a methanogenic enzyme with an unusual quarternary structure. *J. Mol. Biol.* 332:1047–57
39. Hamann N, Mander GJ, Shokes JE, Scott RA, Bennati M, Hedderich R. 2007. A cysteine-rich CCG domain contains a novel [4Fe-4S] cluster binding motif as deduced from studies with subunit B of heterodisulfide reductase from *Methanothermobacter marburgensis*. *Biochemistry* 46:12875–85
40. Harms U, Thauer RK. 1996. The corrinoid-containing 23-kDa subunit MtrA of the energy-conserving N^5-methyltetrahydromethanopterin:coenzyme M methyltransferase complex from *Methanobacterium thermoautotrophicum*: EPR spectroscopic evidence for a histidine residue as a cobalt ligand of the cobamide. *Eur. J. Biochem.* 241:149–54
41. Harms U, Weiss DS, Gärtner P, Linder D, Thauer RK. 1995. The energy conserving N^5-methyltetrahydromethanopterin:coenzyme M methyltransferase complex from *Methanobacterium thermoautotrophicum* is composed of eight different subunits. *Eur. J. Biochem.* 228:640–48
42. Haroon MF, Hu SH, Shi Y, Imelfort M, Keller J, et al. 2013. Anaerobic oxidation of methane coupled to nitrate reduction in a novel archaeal lineage. *Nature* 500:567–70
43. Hay S, Pudney CR, McGrory TA, Pang J, Sutcliffe MJ, Scrutton NS. 2009. Barrier compression enhances an enzymatic hydrogen-transfer reaction. *Angew. Chem. Int. Ed.* 48:1452–54
44. Hedderich R, Albracht SPJ, Linder D, Koch J, Thauer RK. 1992. Isolation and characterization of polyferredoxin from *Methanobacterium thermoautotrophicum*—the *mvhB* gene-product of the methylviologen-reducing hydrogenase operon. *FEBS Lett.* 298:65–68
45. Hedderich R, Berkessel A, Thauer RK. 1989. Catalytic properties of the heterodisulfide reductase involved in the final step of methanogenesis. *FEBS Lett.* 255:67–71
46. Hedderich R, Berkessel A, Thauer RK. 1990. Purification and properties of heterodisulfide reductase from *Methanobacterium thermoautotrophicum* (strain Marburg). *Eur. J. Biochem.* 193:255–61
47. Hedderich R, Koch J, Linder D, Thauer RK. 1994. The heterodisulfide reductase from *Methanobacterium thermoautotrophicum* contains sequence motifs characteristic of pyridine-nucleotide-dependent thioredoxin reductases. *Eur. J. Biochem.* 225:253–61
48. Heiden S, Hedderich R, Setzke E, Thauer RK. 1994. Purification of a two-subunit cytochrome-*b*-containing heterodisulfide reductase from methanol-grown *Methanosarcina barkeri*. *Eur. J. Biochem.* 221:855–61
49. Hemmann JL, Saurel O, Ochsner AM, Stodden BK, Kiefer P, et al. 2016. The one-carbon carrier methylofuran from *Methylobacterium extorquens* AM1 contains a large number of α- and γ-linked glutamic acid residues. *J. Biol. Chem.* 291:9042–51
50. Hemmann JL, Wagner T, Shima S, Vorholt JA. 2019. Methylofuran is a prosthetic group of the formyltransferase/hydrolase complex and shuttles one-carbon units between two active sites. *PNAS* 116:25583–90
51. Hiromoto T, Ataka K, Pilak O, Vogt S, Stagni MS, et al. 2009. The crystal structure of C176A mutated [Fe]-hydrogenase suggests an acyl-iron ligation in the active site iron complex. *FEBS Lett.* 583:585–90

52. Hochheimer A, Hedderich R, Thauer RK. 1998. The formylmethanofuran dehydrogenase isoenzymes in *Methanobacterium wolfei* and *Methanobacterium thermoautotrophicum*: induction of the molybdenum isoenzyme by molybdate and constitutive synthesis of the tungsten isoenzyme. *Arch. Microbiol.* 170:389–93
53. Hochheimer A, Linder D, Thauer RK, Hedderich R. 1996. The molybdenum formylmethanofuran dehydrogenase operon and the tungsten formylmethanofuran dehydrogenase operon from *Methanobacterium thermoautotrophicum*: structures and transcriptional regulation. *Eur. J. Biochem.* 242:156–62
54. Hochheimer A, Schmitz RA, Thauer RK, Hedderich R. 1995. The tungsten formylmethanofuran dehydrogenase from *Methanobacterium thermoautotrophicum* contains sequence motifs characteristic for enzymes containing molybdopterin dinucleotide. *Eur. J. Biochem.* 234:910–20
55. Huang G, Wagner T, Demmer U, Warkentin E, Ermler U, Shima S. 2020. The hydride transfer process in NADP-dependent methylene-tetrahydromethanopterin dehydrogenase. *J. Mol. Biol.* 432:2042–54
56. Huang G, Wagner T, Ermler U, Shima S. 2020. Methanogenesis involves direct hydride transfer from H_2 to an organic substrate. *Nat. Rev. Chem.* 4:213–21
57. Huang GF, Wagner T, Wodrich MD, Ataka K, Bill E, et al. 2019. The atomic-resolution crystal structure of activated [Fe]-hydrogenase. *Nat. Catal.* 2:537–43
58. Kahnt J, Buchenau B, Mahlert F, Krüger M, Shima S, Thauer RK. 2007. Post-translational modifications in the active site region of methyl-coenzyme M reductase from methanogenic and methanotrophic archaea. *FEBS J.* 274:4913–21
59. Kaster A-K, Moll J, Parey K, Thauer RK. 2011. Coupling of ferredoxin and heterodisulfide reduction via electron bifurcation in hydrogenotrophic methanogenic archaea. *PNAS* 108:2981–86
60. Keltjens JT, van der Drift C. 1986. Electron transfer reactions in methanogens (methanogenesis; electron carriers; cell carbon synthesis; energy conservation). *FEMS Microbiol. Rev.* 39:259–303
61. Klein AR, Koch J, Stetter KO, Thauer RK. 1993. Two N^5,N^{10}-methylenetetrahydromethanopterin dehydrogenases in the extreme thermophile *Methanopyrus kandleri*: characterization of the coenzyme-F_{420}-dependent enzyme. *Arch. Microbiol.* 160:186–92
62. Korbas M, Vogt S, Meyer-Klaucke W, Bill E, Lyon EJ, et al. 2006. The iron-sulfur cluster-free hydrogenase (Hmd) is a metalloenzyme with a novel iron binding motif. *J. Biol. Chem.* 281:30804–13
63. Krüger M, Meyerdierks A, Glockner FO, Amann R, Widdel F, et al. 2003. A conspicuous nickel protein in microbial mats that oxidize methane anaerobically. *Nature* 426:878–81
64. Laso-Perez R, Wegener G, Knittel K, Widdel F, Harding KJ, et al. 2016. Thermophilic archaea activate butane via alkyl-coenzyme M formation. *Nature* 539:396–401
65. Lie TJ, Costa KC, Lupa B, Korpole S, Whitman WB, Leigh JA. 2012. Essential anaplerotic role for the energy-converting hydrogenase Eha in hydrogenotrophic methanogenesis. *PNAS* 109:15473–78
66. Livingston DA, Pfaltz A, Schreiber J, Eschenmoser A, Ankelfuchs D, et al. 1984. Factor F_{430} from methanogenic bacteria: structure of the protein-free factor. *Helv. Chim. Acta* 67:334–51
67. Livingston DJ, Fox JA, Ormejohnson WH, Walsh CT. 1987. 8-Hydroxy-5-deazaflavin-reducing hydrogenase from *Methanobacterium thermoautotrophicum*: 2. kinetic and hydrogen-transfer studies. *Biochemistry* 26:4228–37
68. Lyon EJ, Shima S, Boecher R, Thauer RK, Grevels F-W, et al. 2004. Carbon monoxide as an intrinsic ligand to iron in the active site of the iron-sulfur-cluster-free hydrogenase H_2-forming methylenetetrahydromethanopterin dehydrogenase as revealed by infrared spectroscopy. *J. Am. Chem. Soc.* 126:14239–48
69. Lyu Z, Chou CW, Shi H, Wang LL, Ghebreab R, et al. 2018. Assembly of methyl coenzyme M reductase in the methanogenic archaeon *Methanococcus maripaludis*. *J. Bacteriol.* 200:e00746-17
70. Ma K, Thauer RK. 1990. Purification and properties of N^5,N^{10}-methylenetetrahydromethanopterin reductase from *Methanobacterium thermoautotrophicum* (strain Marburg). *Eur. J. Biochem.* 191:187–93
71. Mamat B, Roth A, Grimm C, Ermler U, Tziatzios C, et al. 2002. Crystal structures and enzymatic properties of three formyltransferases from archaea: environmental adaptation and evolutionary relationship. *Protein Sci.* 11:2168–78
72. Mcbride BC, Wolfe RS. 1971. New coenzyme of methyl transfer, coenzyme M. *Biochemistry* 10:2317–24
73. Miller DV, Ruhlin M, Ray WK, Xu HM, White RH. 2017. N^5,N^{10}-Methylenetetrahydromethanopterin reductase from *Methanocaldococcus jannaschii* also serves as a methylglyoxal reductase. *FEBS Lett.* 591:2269–78

74. Mills DJ, Vitt S, Strauss M, Shima S, Vonck J. 2013. De novo modeling of the F_{420}-reducing [NiFe]-hydrogenase from a methanogenic archaeon by cryo-electron microscopy. *eLife* 2:e00218
75. Möller-Zinkhan D, Börner G, Thauer RK. 1989. Function of methanofuran, tetrahydromethanopterin, and coenzyme F_{420} in *Archaeoglobus fulgidus*. *Arch. Microbiol*. 152:362–68
76. Nayak DD, Liu A, Agrawal N, Rodriguez-Carerro R, Shi-Hui D, et al. 2020. Functional interactions between posttranslationally modified amino acids of methyl-coenzyme M reductase in *Methanosarcina acetivorans*. *PLOS Biol*. 18:e3000507. **https://doi.org/10.1371/journal.pbio.3000507**
77. Nayak DD, Mahanta N, Mitchell DA, Metcalf WW. 2017. Post-translational thioamidation of methyl-coenzyme M reductase, a key enzyme in methanogenic and methanotrophic Archaea. *eLife* 6:e29218
78. Nayak DD, Metcalf WW. 2017 Cas9-mediated genome editing in the methanogenic archaeon *Methanosarcina acetivorans*. *PNAS* 114:2976–81
79. Nazaries L, Murrell JC, Millard P, Baggs L, Singh BK. 2013. Methane, microbes and models: fundamental understanding of the soil methane cycle for future predictions. *Environ. Microbiol.* 15:2395–417
80. Noll KM, Rinehart KL, Tanner RS, Wolfe RS. 1986. Structure of component-B (7-mercaptoheptanoylthreonine phosphate) of the methylcoenzyme M methylreductase system of *Methanobacterium thermoautotrophicum*. *PNAS* 83:4238–42
81. Pan H-J, Huang G, Wodrich MD, Tirani FF, Ataka K, et al. 2019. A catalytically active [Mn]-hydrogenase incorporating a non-native metal cofactor. *Nat. Chem.* 11:669–75
82. Pelmenschikov V, Blomberg MRA, Siegbahn PEM, Crabtree RH. 2002. A mechanism from quantum chemical studies for methane formation in methanogenesis. *J. Am. Chem. Soc.* 124:4039–49
83. Pereira IAC, Ramos AR, Grein F, Marques MC, da Silva SM, Venceslau SS. 2011. A comparative genomic analysis of energy metabolism in sulfate reducing bacteria and archaea. *Front. Microbiol.* 2:69
84. Pfaltz A, Livingston DA, Jaun B, Diekert G, Thauer RK, Eschenmoser A. 1985. Factor F_{430} from methanogenic bacteria: on the nature of the isolation artifacts of F_{430}, a contribution to the chemistry of F_{430} and the conformational stereochemistry of the ligand periphery of hydroporphinoid nickel(II) complexes. *Helv. Chim. Acta* 68:1338–58
85. Pilak O, Mamat B, Vogt S, Hagemeier CH, Thauer RK, et al. 2006. The crystal structure of the apoenzyme of the iron-sulphur cluster-free hydrogenase. *J. Mol. Biol.* 358:798–809
86. Prakash D, Wu Y, Suh S-J, Duin EC. 2014. Elucidating the process of activation of methyl-coenzyme M reductase. *J. Bacteriol.* 196:2491–98
87. Rospert S, Böcher R, Albracht SPJ, Thauer RK. 1991. Methyl-coenzyme-M reductase preparations with high specific activity from H_2-preincubated cells o*f Methanobacterium thermoautotrophicum*. *FEBS Lett*. 291:371–75
88. Saunois M, Bousquet P, Poulter B, Peregon A, Ciais P, et al. 2016. The global methane budget 2000–2012. *Earth Syst. Sci. Data* 8:697–751
89. Schaefer H, Mikaloff Fletcher SE, Veidt C, Lassey KR, Brailsford GW, et al. 2016. A 21st-century shift from fossil-fuel to biogenic methane emissions indicated by $^{13}CH_4$. *Science* 352:80–84
90. Scheller S, Goenrich M, Boecher R, Thauer RK, Jaun B. 2010. The key nickel enzyme of methanogenesis catalyses the anaerobic oxidation of methane. *Nature* 465:606–8
91. Schmitz RA, Albracht SPJ, Thauer RK. 1992. A molybdenum and a tungsten isoenzyme of formylmethanofuran dehydrogenase in the thermophilic archaeon *Methanobacterium wolfei*. *Eur. J. Biochem*. 209:1013–18
92. Schmitz RA, Albracht SPJ, Thauer RK. 1992. Properties of the tungsten-substituted molybdenum formylmethanofuran dehydrogenase from *Methanobacterium wolfei*. *FEBS Lett*. 309:78–81
93. Selmer T, Kahnt J, Goubeaud M, Shima S, Grabarse W, et al. 2000. The biosynthesis of methylated amino acids in the active site region of methyl-coenzyme M reductase. *J. Biol. Chem*. 275:3755–60
94. Setzke E, Hedderich R, Heiden S, Thauer RK. 1994. H_2:heterodisulfide oxidoreductase complex from *Methanobacterium thermoautotrophicum*: composition and properties. *Eur. J. Biochem*. 220:139–48
95. Shima S. 2016. The biological methane-forming reaction: mechanism confirmed through spectroscopic characterization of a key intermediate. *Angew. Chem. Int. Ed.* 55:13648–49
96. Shima S, Chen D, Xu T, Wodrich MD, Fujishiro T, et al. 2015. Reconstitution of [Fe]-hydrogenase using model complexes. *Nat. Chem.* 7:995–1002

97. Shima S, Ermler U. 2011. Structure and function of [Fe]-hydrogenase and its iron-guanylylpyridinol (FeGP) cofactor. *Eur. J. Inorg. Chem.* 2011:963–72
98. Shima S, Goubeaud M, Vinzenz D, Thauer RK, Ermler U. 1997. Crystallization and preliminary X-ray diffraction studies of methyl-coenzyme M reductase from *Methanobacterium thermoautotrophicum*. *J. Biochem.* 121:829–30
99. Shima S, Krueger M, Weinert T, Demmer U, Kahnt J, et al. 2012. Structure of a methyl-coenzyme M reductase from Black Sea mats that oxidize methane anaerobically. *Nature* 481:98–101
100. Shima S, Lyon EJ, Sordel-Klippert MS, Kauss M, Kahnt J, et al. 2004. The cofactor of the iron-sulfur cluster free hydrogenase Hmd: structure of the light-inactivation product. *Angew. Chem. Int. Ed.* 43:2547–51
101. Shima S, Lyon EJ, Thauer RK, Mienert B, Bill E. 2005. Mössbauer studies of the iron-sulfur cluster-free hydrogenase: the electronic state of the mononuclear Fe active site. *J. Am. Chem. Soc.* 127:10430–35
102. Shima S, Pilak O, Vogt S, Schick M, Stagni MS, et al. 2008. The crystal structure of [Fe]-hydrogenase reveals the geometry of the active site. *Science* 321:572–75
103. Shima S, Schick M, Kahnt J, Ataka K, Steinbach K, Linne U. 2012. Evidence for acyl-iron ligation in the active site of [Fe]-hydrogenase provided by mass spectrometry and infrared spectroscopy. *Dalton Trans.* 41:767–71
104. Shima S, Thauer RK. 2001. Tetrahydromethanopterin-specific enzymes from *Methanopyrus kandleri*. *Methods Enzymol.* 331:317–53
105. Shima S, Thauer RK, Ermler U, Durchschlag H, Tziatzios C, Schubert D. 2000. A mutation affecting the association equilibrium of formyltransferase from the hyperthermophilic *Methanopyrus kandleri* and its influence on the enzyme's activity and thermostability. *Eur. J. Biochem.* 267:6619–23
106. Shima S, Tziatzios C, Schubert D, Fukada H, Takahashi K, et al. 1998. Lyotropic-salt-induced changes in monomer/dimer/tetramer association equilibrium of formyltransferase from the hyperthermophilic *Methanopyrus kandleri* in relation to the activity and thermostability of the enzyme. *Eur. J. Biochem.* 258:85–92
107. Shima S, Warkentin E, Grabarse W, Sordel M, Wicke M, et al. 2000. Structure of coenzyme F_{420} dependent methylenetetrahydromethanopterin reductase from two methanogenic archaea. *J. Mol. Biol.* 300:935–50
108. Te Brömmelstroet BW, Hensgens CMH, Geerts WJ, Keltjens JT, Vanderdrift C, Vogels GD. 1990. Purification and properties of 5,10-methenyltetrahydromethanopterin cyclohydrolase from *Methanosarcina barkeri*. *J. Bacteriol.* 172:564–71
109. Te Brömmelstroet BW, Hensgens CMH, Keltjens JT, Vanderdrift C, Vogels GD. 1991. Purification and characterization of coenzyme F_{420}-dependent 5,10-methylenetetrahydromethanopterin dehydrogenase from *Methanobacterium thermoautotrophicum* Strain ΔH. *Biochim. Biophys. Acta Gen. Subj.* 1073:77–84
110. Tersteegen A, Hedderich R. 1999. *Methanobacterium thermoautotrophicum* encodes two multisubunit membrane-bound [NiFe] hydrogenases—transcription of the operons and sequence analysis of the deduced proteins. *Eur. J. Biochem.* 264:930–43
111. Thauer RK. 2012. The Wolfe cycle comes full circle. *PNAS* 109:15084–85
112. Thauer RK. 2019. Methyl (alkyl)-coenzyme M reductases: nickel F_{430}-containing enzymes involved in anaerobic methane formation and in anaerobic oxidation of methane or of short chain alkanes. *Biochemistry* 58(25):5198–220
113. Thauer RK, Kaster AK, Goenrich M, Schick M, Hiromoto T, Shima S. 2010. Hydrogenases from methanogenic archaea, nickel, a novel cofactor, and H_2 storage. *Annu. Rev. Biochem.* 79:507–36
114. Thauer RK, Kaster AK, Seedorf H, Buckel W, Hedderich R. 2008. Methanogenic archaea: ecologically relevant differences in energy conservation. *Nat. Rev. Microbiol.* 6:579–91
115. Thauer RK, Klein AR, Hartmann GC. 1996. Reactions with molecular hydrogen in microorganisms: evidence for a purely organic hydrogenation catalyst. *Chem. Rev.* 96:3031–42
116. Thauer RK, Shima S. 2008. Methane as fuel for anaerobic microorganisms. *Ann. N. Y. Acad. Sci.* 1125:158–70
117. Tian H, Lu C, Ciais P, Michalak AM, Canadell JG, et al. 2016. The terrestrial biosphere as a net source of greenhouse gases to the atmosphere. *Nature* 531:225–28

118. Upadhyay V, Ceh K, Tumulka F, Abele R, Hoffmann J, et al. 2016. Molecular characterization of methanogenic N^5-methyl-tetrahydromethanopterin:coenzyme M methyltransferase. *Biochim. Biophys. Acta Biomembr.* 1858:2140–44
119. Upadhyay V, Demmer U, Warkentin E, Moll J, Shima S, Ermler U. 2012. Structure and catalytic mechanism of N^5,N^{10}-methenyltetrahydromethanopterin cyclohydrolase. *Biochemistry* 51:8435–43
120. Vitt S, Ma K, Warkentin E, Moll J, Pierik AJ, et al. 2014. The F_{420}-reducing [NiFe]-hydrogenase complex from *Methanothermobacter marburgensis*, the first X-ray structure of a group 3 family member. *J. Mol. Biol.* 426:2813–26
121. Vogt S, Lyon EJ, Shima S, Thauer RK. 2008. The exchange activities of [Fe] hydrogenase (iron-sulfur-cluster-free hydrogenase) from methanogenic archaea in comparison with the exchange activities of [FeFe] and [NiFe] hydrogenases. *J. Biol. Inorg. Chem.* 13:97–106
122. Wagner T, Ermler U, Shima S. 2016. MtrA of the sodium ion pumping methyltransferase binds cobalamin in a unique mode. *Sci. Rep.* 6:28226
123. Wagner T, Ermler U, Shima S. 2016. The methanogenic CO_2 reducing-and-fixing enzyme is bifunctional and contains 46 [4Fe-4S] clusters. *Science* 354:114–17
124. Wagner T, Kahnt J, Ermler U, Shima S. 2016. Didehydroaspartate modification in methyl-coenzyme M reductase catalyzing methane formation. *Angew. Chem. Int. Ed.* 55:10630–33
125. Wagner T, Koch J, Ermler U, Shima S. 2017. Methanogenic heterodisulfide reductase (HdrABC-MvhAGD) uses two noncubane [4Fe-4S] clusters for reduction. *Science* 357:699–703
126. Wagner T, Wegner C-E, Kahnt J, Ermler U, Shima S. 2017. Phylogenetic and structural comparisons of the three types of methyl-coenzyme M reductase from *Methanococcales* and *Methanobacteriales*. *J. Bacteriol.* 199:e00197-17
127. Weiss DS, Gärtner P, Thauer RK. 1994. The energetics and sodium-ion dependence of N^5-methyltetrahydromethanopterin:coenzyme M methyltransferase studied with cob(I)alamin as methyl acceptor and methylcob(III)alamin as methyl donor. *Eur. J. Biochem.* 226:799–809
128. White RH. 1998. Methanopterin biosynthesis: methylation of the biosynthetic intermediates. *Biochim. Biophys. Acta Gen. Subj.* 1380:257–67
129. Wongnate T, Ragsdale SW. 2015. The reaction mechanism of methyl-coenzyme M reductase: how an enzyme enforces strict binding order. *J. Biol. Chem.* 290:9322–34
130. Wongnate T, Sliwa D, Ginovska B, Smith D, Wolf MW, et al. 2016. The radical mechanism of biological methane synthesis by methyl-coenzyme M reductase. *Science* 352:953–58
131. Zhou YZ, Dorchak AE, Ragsdale SW. 2013. In vivo activation of methyl-coenzyme M reductase by carbon monoxide. *Front. Microbiol.* 4:69
132. Zirngibl C, Van Dongen W, Schwörer B, von Bünau R, Richter M, et al. 1992. H_2-forming methylenetetrahydromethanopterin dehydrogenase, a novel type of hydrogenase without iron-sulfur clusters in methanogenic archaea. *Eur. J. Biochem.* 208:511–20

Annual Review of Microbiology
Volume 74, 2020

Contents